

# Conformation and location of amorphous and semi-crystalline regions in C-type starch granules revealed by SEM, NMR and XRD

Shujun Wang<sup>a</sup>, Jinglin Yu<sup>b,\*</sup>, Jiugao Yu<sup>c</sup>

<sup>a</sup> College of Pharmaceutical Science and Technology, Tianjin University, Tianjin 300072, China

<sup>b</sup> College of Traditional Chinese Medicine, Tianjin University of Traditional Chinese Medicine, Tianjin 300193, China

<sup>c</sup> College of Science, Department of Chemistry, Tianjin University, Tianjin 300072, China

Received 7 October 2007; received in revised form 10 November 2007; accepted 25 January 2008

## Abstract

The conformations and locations of amorphous and semi-crystalline regions in C-type starch granules from Chinese yam were evaluated by a combination of morphology and spectroscopy studies during acid hydrolysis. Scanning electron micrographs showed that amorphous or less crystalline areas were essentially located in the centre part of C-type starch granules, whereas the semi-crystalline and amorphous growth rings were found mainly in the outer part of the granules. <sup>13</sup>C cross-polarization magic angle spinning NMR (<sup>13</sup>C CP/MAS NMR) showed that amorphous regions were hydrolyzed faster than the crystalline ones. In addition, B-type polymorphs were shown to be hydrolyzed more rapidly than A-types. Powder X-ray diffraction (XRD) also revealed that the B-polymorph was hydrolyzed more rapidly than the A-type. XRD showed that the amorphous or less crystalline areas were mainly located in the core of starch granules, while the amorphous growth rings are distributed toward the outside of the granules and alternatively arranged with semi-crystalline growth rings. The amorphous or less crystalline areas predominantly consisted of the B-polymorph whereas the outer semi-crystalline and amorphous growth rings were mostly composed of the A-polymorph.

© 2008 Elsevier Ltd. All rights reserved.

**Keywords:** C-type starch; Semi-crystalline; Amorphous; Polymorphs; Growth rings

## 1. Introduction

Starch, the major plant storage polysaccharide, is deposited in semi-crystalline granular form. From a molecular perspective, it mainly consists of two types of  $\alpha$ -linked D-glucosyl homopolymers, namely amylose and amylopectin. Amylose and amylopectin are packed into granules, which are part crystalline and part amorphous in structure. It is hypothesized that the crystallites are composed of parallel, left-handed double helices formed from the short external amylopectin chains (Buléon, Colomna, Planchot, & Ball, 1998; Buléon et al., 1997; Jane, Kasemsuwan, Leas, Zobel, & Robyt, 1994; Oostergetel & van Bruggen, 1989). Two

types of crystallites, or polymorph structures, A and B, are thought to have the same double helical conformation but different packing arrangement and different intracrystalline water content in native starch granules (Oostergetel & van Bruggen, 1989; Sarko & Wu, 1978; Vermeylen, Godearis, Reynaers, & Delcour, 2004). Starches from different origins have either A (e.g., maize), B (e.g., potato), or both A and B (e.g., pea or Chinese yam) types of polymorph (Wang et al., 2006a, 2006b; Wang, Yu, Gao, Liu, & Xiao, 2006c).

The location of the A- and B-polymorphs in C-type starch has been debated for a long time. Bogracheva, Morris, Ring, and Hedley (1998) and Buléon et al. (1998) reported the location of the polymorphic crystalline components of C-type smooth pea starch granules by polarized light microscopy during gelatinization in excess salt solution and by synchrotron microfocus mapping, respectively. They concluded that the centre of the granules consisted

\* Corresponding author.

E-mail address: [edwinwa@hotmail.com](mailto:edwinwa@hotmail.com) (S. Wang).

mainly of the B-polymorph whereas the A-polymorph was located toward the outside of the granules. In our previous report, structural characteristics were studied by observing structural changes of C-type starch during acid hydrolysis. SEM showed that acid corrosion firstly occurred in the inner part followed by the outer part of starch granules. B-polymorphism was not detected by X-ray diffraction in the acid-modified starches subjected to 32 days of hydrolysis. Preliminary results showed B-polymorphism exists mostly in the core of the C-type starch granule and is surrounded by the A-polymorph. Amorphous regions are essentially composed of the B-polymorph while the crystalline regions are chiefly made up of the A-polymorph (Wang, Yu, Yu, Chen, & Pang, 2007; Wang, Yu, & Gao, et al., 2007).

Enzymic and acid hydrolysis revealed the presence of alternating, readily degradable, and more resistant shells (120–400 nm) in the starch granules (French, 1984). The more resistant shell, named the semi-crystalline shell, is considered to be more “crystalline” than the rapidly degradable “amorphous” shell (Jenkins et al., 1994). This so-called onion-like structure, with more or less concentric growth rings, is readily visible by optical and electron microscopy (Buttrose, 1960; Nikuni & Whistler, 1957). According to Cameron and Donald (1992), the amorphous growth ring is at least as thick as the semi-crystalline one. Based on atomic force microscopy (AFM) measurements, Dang and Copeland (2003) suggested that the growth rings in rice are approximately 400 nm apart. Most of the detailed research on granule structure has focused on the nature of the alternating amorphous and crystalline layers or rings, while little work has been directed to the less well-organized hilum region or its neighboring region. Indeed, the intermediate core between the hilum and the alternating growth rings is little known (Ziegler, Creek, & Runt, 2005).

We therefore aimed to further see the conformation and location of the amorphous and semi-crystalline regions, the location of the B-polymorph and A-polymorph, in C-type Chinese yam starch during acid hydrolysis with the use of Environment Scanning Electron Microscopy (ESEM), Solid-state  $^{13}\text{C}$  CP/MAS NMR, and powder X-ray diffraction (XRD).

## 2. Experimental section

### 2.1. Sample preparation

Samples of C-type Rhizoma *Dioscorea* starch were obtained from dried Rhizoma of *Dioscorea opposita* Thunb. cv. RiBenBai (*D. RBB*) in our laboratory. The acid-modified starch was prepared according to the methods described in previous work (Wang, Yu, & Yu, et al., 2007; Wang, Yu, & Gao, et al., 2007). Ten grams (dry basis) of native *D. RBB* starch was hydrolyzed by suspending in 400 ml of 2.2 mol/l HCl solution at 35 °C for 2, 4, 8, 16, 32 and 40 days with stirring once a day. After

hydrolysis, the suspension was filtered with a G4 type acid funnel by vacuum filtration. The insoluble residue was washed several times with distilled water to neutrality. The resulting filter cake was again washed 2–4 times with acetone. The resulting acid-thinned starch was dried at the room temperature overnight (air stream). All the specimens were stored in a desiccator where a saturated solution of NaCl maintained a constant humidity atmosphere (relative humidity RH = 75%) for one week before measurements.

### 2.2. SEM observations

The granular structure changes were analyzed by using an environmental scanning electron microscope (ESEM, Philips XL-3, Holland) at 20 kV. Acid-thinned starch samples were suspended in acetone to obtain a 1% suspension. One drop of the starch-acetone suspension was applied on an aluminium stub using double-sided adhesive tape and the starch was coated with gold powder to avoid charging under the electron beam after the acetone was volatilized.

### 2.3. X-ray diffraction analysis

The X-ray diffraction pattern was recorded with a cobalt anode X-ray tube (Co  $\text{K}\alpha$  radiation,  $\lambda = 0.178901$  nm) using a Panalytical X'Pert Pro X-ray powder diffractometer (Panalytical, Holland). The starch powders were packed tightly in sample holders. Each sample was exposed to the X-ray beam at 45 kV and 30 mA. The scanning region of the diffraction angle ( $2\theta$ ) was from 4° to 35° at 0.0170° step size with a scan step time of 30.8451 s.

### 2.4. Solid-state $^{13}\text{C}$ CP/MAS NMR analysis

High-resolution solid-state  $^{13}\text{C}$  CP/MAS NMR experiments were conducted using a Varian Unity plus 300WB spectrometer at resonance frequencies of 75 MHz. NMR spectra were observed under cross-polarization (CP), magic angle sample spinning (MAS) and high power decoupling (DD) conditions. Samples were spun at the magic angle (54.5° or 54.7°). A magic-angle spinning rate of 2.5 kHz and decoupling field of 61 kHz were used. The 90° pulse width was 4  $\mu\text{s}$  with a recycle time of 5 s. A contact time of 1 ms was used for all the samples; spectral width was 20 kHz; acquisition time, 27 ms. Each sample was packed into a 7 mm MAS sample rotor with tight push-fitting caps. The rotor held 200–240 mg of starch sample. Spectra were referenced to external  $\text{Me}_4\text{Si}$  via the low field resonance of adamantane (38.6 ppm). About 10,000 scans were accumulated for each spectra to obtain a satisfactory signal-noise ratio. A polynomial baseline was manually corrected where necessary after Fourier transformation and phasing.

### 3. Results and discussion

#### 3.1. Scanning electron microscopy (SEM)

Scanning electron micrographs of native *D. RBB* starch and acid-modified starches are presented in Fig. 1. The granular size of the native starch ranged from 15 to 40  $\mu\text{m}$  in diameter. Granules were oval to irregular in shape with smooth surfaces with no evidence of indentations, fissures or pores (Fig. 1a<sub>1</sub> and a<sub>2</sub>). After 2, 4 and 8 days of hydrolysis, no clear flaws or fractures could be observed on the surface of most of the starch granules, whether at 1000  $\times$  magnification or at 2000  $\times$  magnification (Fig. 1b<sub>1</sub>–d<sub>2</sub>). The granular size of starch is essentially invariable. Most of the starch granules still showed the smooth surface with a few fragments when they are subjected to 16 days of hydrolysis (Fig. 1e<sub>1</sub> and e<sub>2</sub>). The striking change is that some starch granules were shrunken with the degradation of the interior of granules. After further hydrolysis for 32 days, exocorrosion occurred all over the granule surface (Fig. 1f<sub>1</sub>). Some small fragments hydrolyzed from the outer layer of starch granules were visible in Fig. 1f<sub>2</sub> (indicated by black arrows). Although most of the starch granules still remained relatively intact, they became more crimped due to the severe corrosion of the inner part of granules. After prolonged hydrolysis for 40 days, more severe exocorrosion resulted in the fracture of most starch granules (Fig. 1g<sub>1</sub> and g<sub>2</sub>). When observing the cracked granules, we discovered some clear cavities in the centre of granules (Fig. 1g<sub>3</sub> and g<sub>4</sub>, indicated by black arrows). This indicates that the interior of starch granules is essentially hollow before they are fractured.

According to the changes in the morphology of starch granules during acid hydrolysis, it could be concluded that starch granules are substantial from hilum to outer surface and that some cavities will be formed at the interior of starch granules with the powers of hydrolysis. Most of the acid hydrolysis data proved that the acid attacked amorphous areas more rapidly than crystalline ones, which are less accessible to  $\text{H}_3\text{O}^+$  ions (Jayakody & Hoover, 2002; Jenkins & Donald, 1997). This rule was further confirmed by the recent results of Putaux, Molina-Boisseau, Momaour, and Dufresne (2003) who reported also that the degradation of the crystalline growth rings, although slow, and that of the amorphous areas are concomitant. The starch granules remain relatively intact and the crystalline fragments are not detected until after 16 days of hydrolysis. This reveals that the amorphous areas or less crystalline areas are preferentially degraded during the first step of hydrolysis. Considering the cavities formed in the centre of starch granules during the first stage of hydrolysis, as well as the hydrolysis rule, one could conclude that partially amorphous or less crystalline areas of C-type *D. RBB* starch mostly occur in the core part of starch granules and are surrounded by amorphous and semi-crystalline growth rings. The schematic drawing of starch granules is shown in Fig. 2.

It is generally accepted that starch granules consist of concentric shells, often called alternating amorphous and semi-crystalline growth rings (French, 1984; Jenkins et al., 1994). However, Ridout, Parker, Hedley, Bogracheva, and Morris (2004) recently reported that the amorphous and crystalline growth rings of pea starch granules viewed by atomic force microscopy were both partially crystalline in character. According to the model of growth rings, the amorphous areas of starch granules are believed to be composed of two parts: amorphous growth rings and amorphous lamellae constituting the semi-crystalline growth rings. The model presented in this study (Fig. 2) are somewhat inconsistent with the currently accepted model. However, another model (Ziegler et al., 2005) of the hilum and its surrounding semi-crystalline core, with a lower degree of organization relative to the more crystalline layers at the periphery were in agreement with our suggested model. They considered that the observable region between hilum and semi-crystalline growth rings is a core of less crystalline material. Unfortunately, the intermediate region between hilum and growth rings were not confirmed to be a less crystalline phase or amorphous phase in this study.

#### 3.2. $^{13}\text{C}$ CP/MAS NMR

The  $^{13}\text{C}$  CP/MAS NMR patterns for native and acid-thinned starches at various hydrolysis times are shown in Fig. 3. As for the C-type starch, the resonances in the spectrum could depend on the proportion of A- or B-type polymorph in the sample. C-type starch shows triplet C-1 spectra if the A-type polymorph is predominant. If the B-type polymorph is greatest in the C-type starch granules, it will yield a two-peak pattern for C-1 signals (Cheetham & Tao, 1998). From Fig. 3a, the three peaks at 101.7, 100.7 and 99.8 ppm for characterizing A-type starch indicates that A-type polymorphs predominate in the native C-type starch. The C-1 (at 103 ppm) and C-4 (at 82.5 ppm) resonances, characteristic for amorphous regions, are clearly present on this pattern. The major signals at 68–78 ppm are collectively associated with C-2, -3, -4 and -5 sites and the resonance at 62.3 ppm is assigned to C-6. Apart from the above broad peaks, the weak peak appears at 94.3 ppm could be attributed to high-energy, twisted conformations remote from those characteristic of single helices (102–103 ppm) and double helices (99–101 ppm). These assignments of the resonances are based on the literature reported chemical shifts (Bogracheva, Wang, & Hedley, 2001; Gidley & Bociek, 1985; Tang & Hills, 2003; Veregin, Fyfe, Marchessault, & Taylor, 1986).

Three striking differences are observed in the  $^{13}\text{C}$  CP/MAS NMR patterns for native and acid-thinned starches. Firstly, the intensity of C-1 and C-4 amorphous resonances (103 and 82.5 ppm) are found to decrease gradually with increasing hydrolysis time and almost disappeared when the hydrolysis time reached 40 days. In general, amorphous compounds give broad resonances as the distribution of

local molecular environments give rise to a broad distribution of chemical shifts for each carbon. Ordered materials show narrower resonances due to more regularity of the environment (Gidley & Bociek, 1985; Veregin et al.,

1986), reflecting the stricter polymer configurations in the ordered parts of starch (Paris, Bizot, Emery, Buzare, & Bu-leon, 1999). The disappearance of the resonances of amorphous components suggests that the amorphous regions in

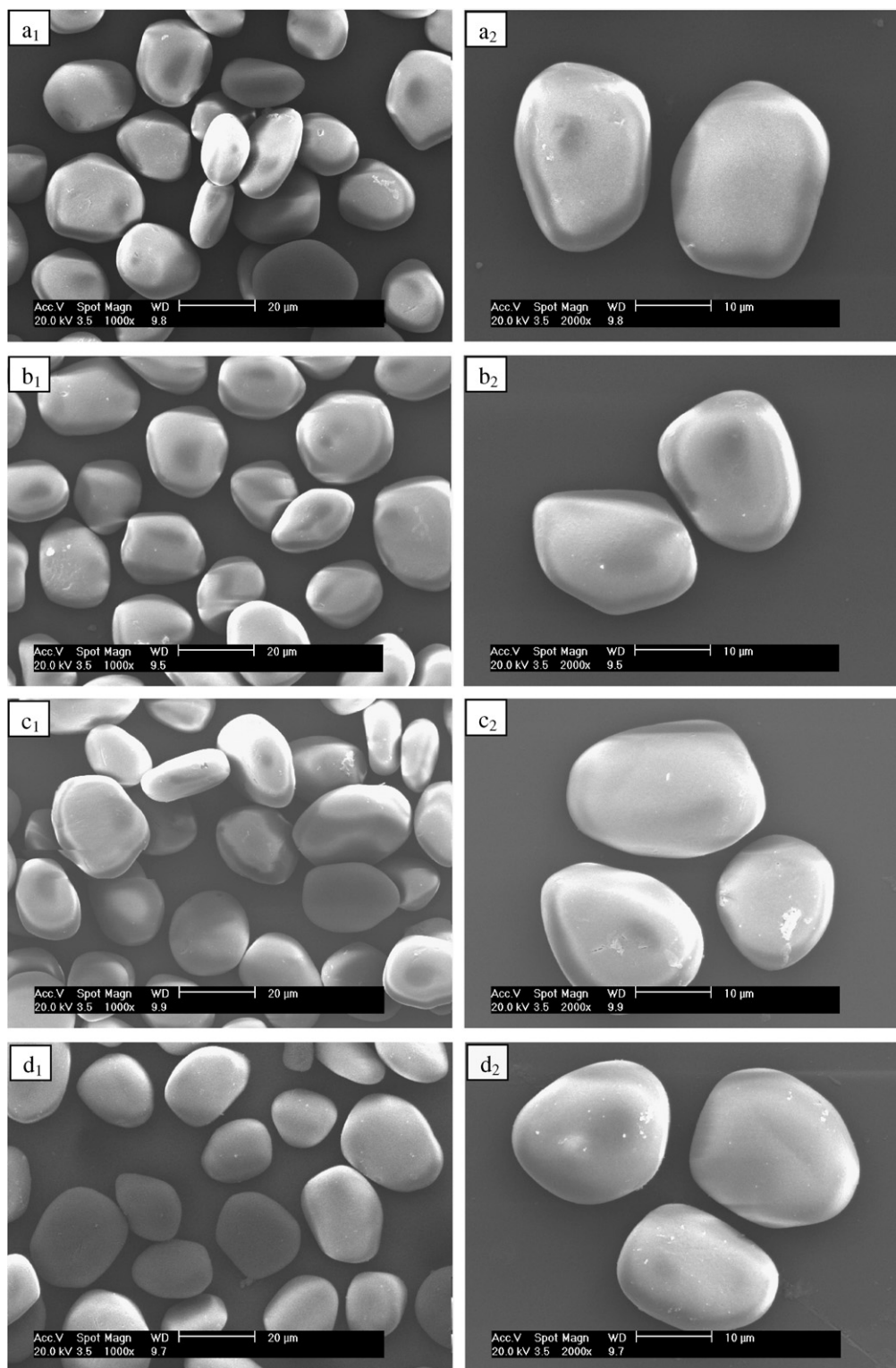


Fig. 1. SEM photographs of native and modified starches. (a<sub>1</sub>) (a<sub>2</sub>) SEM photographs of native starch granules; (b<sub>1</sub>) (b<sub>2</sub>), (c<sub>1</sub>) (c<sub>2</sub>), (d<sub>1</sub>) (d<sub>2</sub>), (e<sub>1</sub>) (e<sub>2</sub>), (f<sub>1</sub>) (f<sub>2</sub>) SEM photographs of starch granules hydrolyzed for 2, 4, 8, 16 and 32 days, respectively; (g<sub>1</sub>) (g<sub>2</sub>) (g<sub>3</sub>) (g<sub>4</sub>) SEM photographs of starch granules hydrolyzed for 40 days.

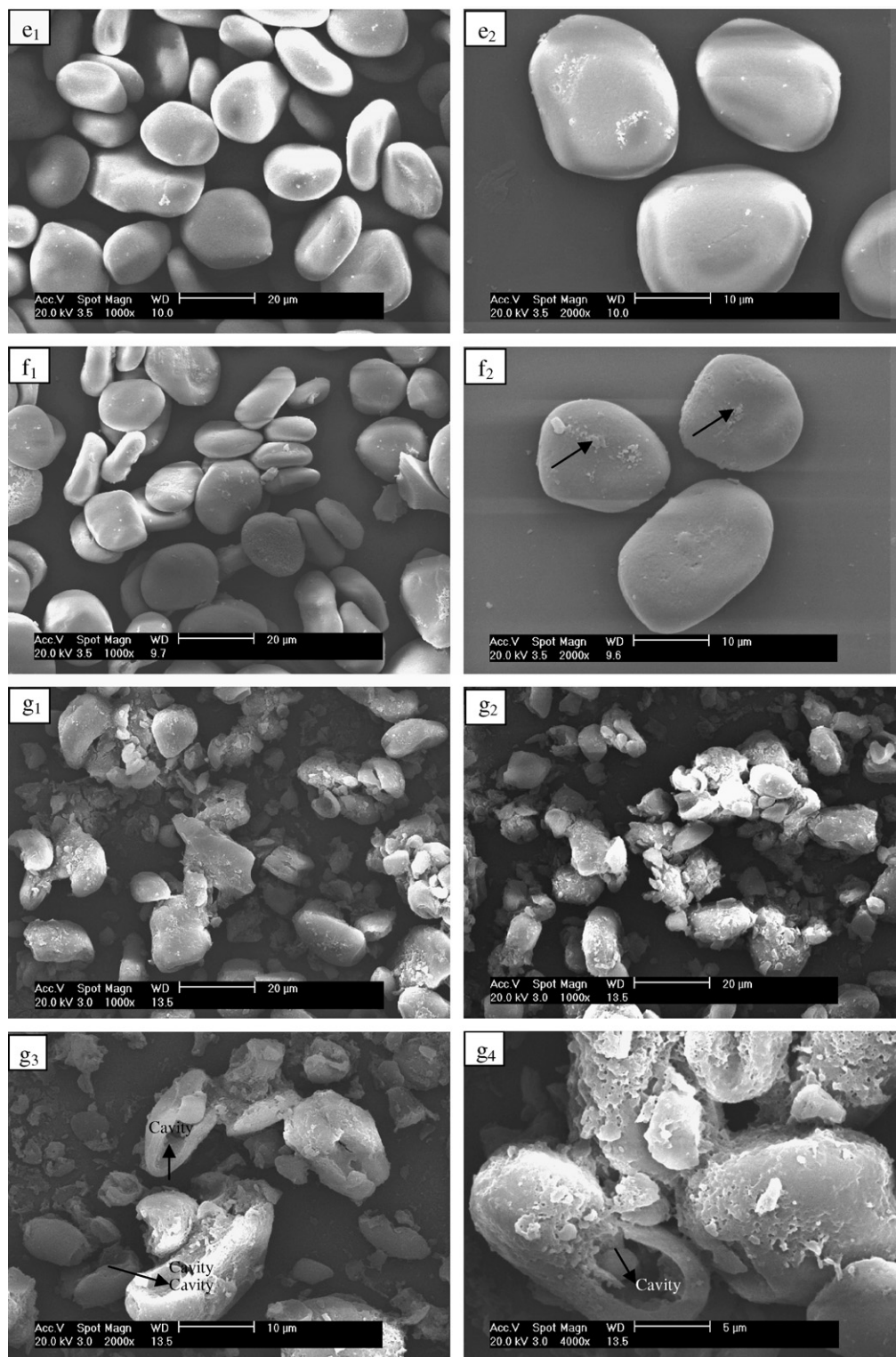


Fig. 1 (continued)

the starch granules are preferentially hydrolyzed or hydrolyzed rapidly, being in agreement with previously reported findings (Atichokudomchai, Varavinit, & Chinachoti, 2004). The second difference is that the characteristic resonances (triplets) for A-type starch become more and more prominent with hydrolysis time prolonging. When the hydrolysis time reached 40 days, the acid-thinned starch

shows a typical  $^{13}\text{C}$  CP/MAS NMR pattern (Fig. 3g) of A-type crystalline (1  $\rightarrow$  4)- $\alpha$ -D-glucan oligomers (derived from debranched glycogen) (Gidley & Bociek, 1985), indicating that the A-type polymorph is absolutely dominant in the acid-thinned starch. This result also reveals that the long-range ordering in starch granules (through regular packing of double helices formed from adjacent branches)

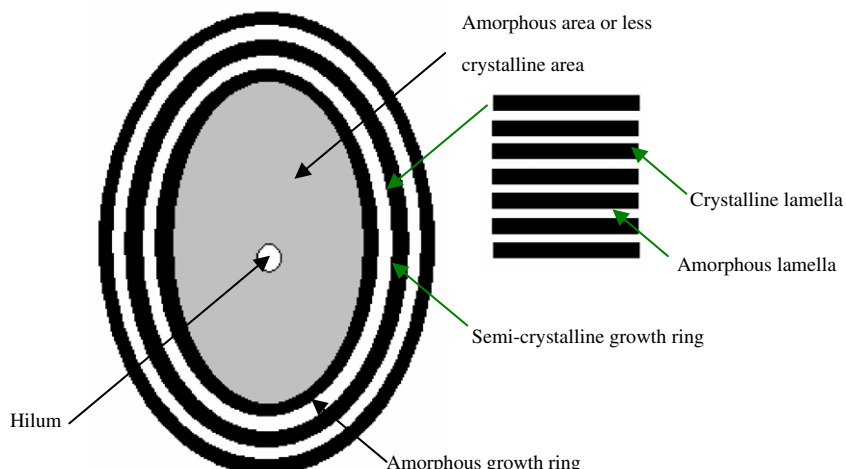


Fig. 2. Schematic drawing of C-type *D. RBB* starch granule structure: hilum (white dot), amorphous area (gray) and semi-crystalline growth rings (crystalline growth rings (black) and amorphous growth rings (white)).

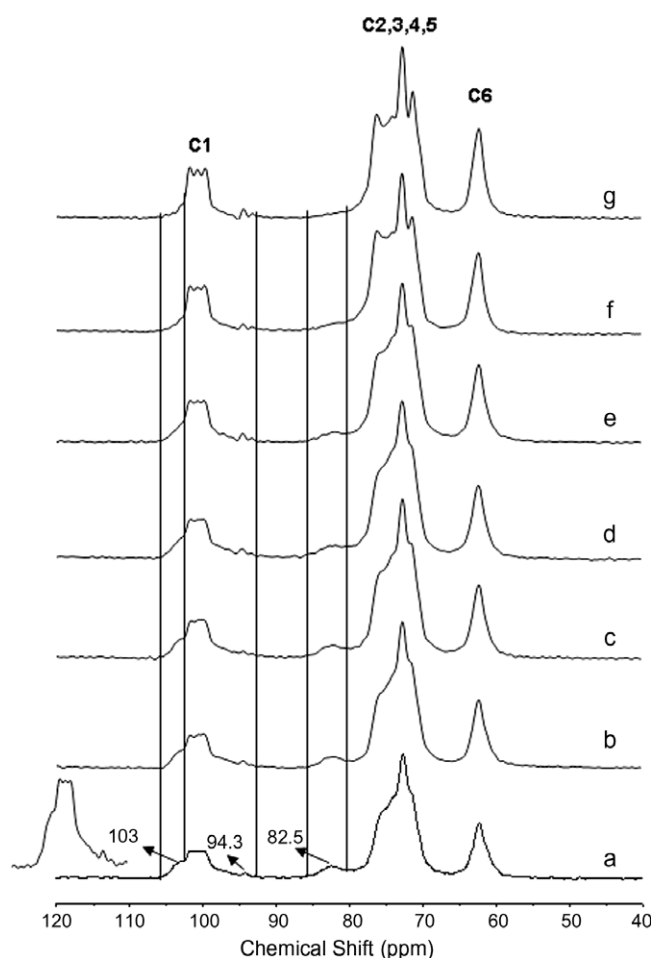


Fig. 3.  $^{13}\text{C}$  CP/MAS NMR spectra of native and acid-thinned starches hydrated at 100% relative humidity. (a) Native starch, (b) 2 days, (c) 4 days, (d) 8 days, (e) 32 days and (f) 40 days.

will be formed from the short chains of similar length developed during the process of hydrolysis. The last notable exception is the resonance changes for C-2, -3, -4 and

-5 during acid hydrolysis. As for C-type native starch granules, three signals could be observed at 72.7 ppm (centre), 71.5 and 76 ppm (two shoulders). The three peaks become better resolved when the hydrolysis time increases step by step. The four well-resolved signals (one crest peak and three shoulder peaks) are observable at 72.7 ppm (centre), 71.2-, 74.2- and 76.2 ppm (three shoulders), also being the typical pattern of A-type starch with high water content (Bogracheva et al., 2001; Paris et al., 1999).

The above three changes in the  $^{13}\text{C}$  CP/MAS NMR patterns between native and acid-modified starches show two important information on the structural changes during acid hydrolysis: (1) the amorphous phase in the starch granule is preferentially degraded; (2) the B-type polymorph

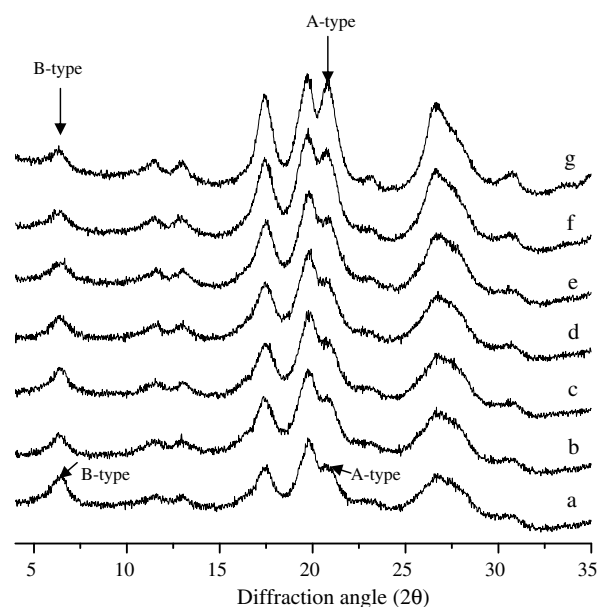


Fig. 4. X-ray powder diffraction spectra of native and acid-modified starches at various hydrolysis times. (a) Native starch, (b) 2 days, (c) 4 days, (d) 8 days, (e) 32 days and (f) 40 days.

in the C-type starch is hydrolyzed first or faster than the A-type.

### 3.3. XRD

The X-ray powder diffraction patterns for both native and acid-thinned starches are shown in Fig. 4. The peak at around  $2\theta$  value of  $6.3^\circ$  is characteristic of a B-type pattern, while those at  $19.7^\circ$ ,  $20.8^\circ$  and  $26.6^\circ$   $2\theta$  are indicative of the A-type pattern, showing that native starch is a typical C-type starch. The decrease in intensity of the peak at  $6.3^\circ$   $2\theta$  and the increase in that of the peak at  $26.6^\circ$   $2\theta$  reveals a decrease in the proportion of B-type polymorph to A-type polymorph. Additionally, the peak at around  $2\theta$  value of  $19.7^\circ$  with a weak shoulder peak ( $20.8^\circ$   $2\theta$ ) splitting into two broad peaks at  $19.7^\circ$  and  $20.8^\circ$  also adds weight to the above idea. This also indicates that the B-type polymorph is hydrolyzed preferentially or more rapidly than the A-type.

## 4. Conclusions

The detailed structural information on C-type starch from Chinese yam was obtained by analyzing the structure of insoluble residues of starch granules. Three important information could be obtained from the experimental results: (1) The amorphous or less crystalline areas are mainly located in the core of starch granules, the amorphous growth rings are distributed toward the outside of the granules and alternatively arranged with semi-crystalline growth rings; (2) B-type allomorph present in C-type starch granules is essentially composed of the amorphous or the less crystalline regions. Whereas the semi-crystalline and amorphous growth rings in the outer part of C-type starch granules predominantly consists of the A-type allomorph. (3) The A- and B-type allomorph coexists in the individual C-type starch granule; B-type allomorph basically exists in the centre part of the granules which is surrounded by the A-type allomorph in the peripheral part of granules.

## Acknowledgments

We acknowledge the financial assistance of Program for *New Century Excellent Scholar in Universities*. We also acknowledge the technical assistance of K. Y. Zhu, T. Xue and F. M. Jin (Tianjin University, Tianjin, China) for the  $^{13}\text{C}$  CP/NMR, SEM and XRD measurements. We also thank Dr. L. Cui and Dr. X. W. Du (Tianjin University, Tianjin, China) for helpful discussions.

## References

Atichokudomchai, N., Varavinit, S., & Chinachoti, P. (2004). A study of ordered structure in acid-modified starch by  $^{13}\text{C}$  CP/MAS solid-state NMR. *Carbohydrate Polymers*, 58, 383–389.

Boggracheva, T. Y., Morris, V. J., Ring, S. G., & Hedley, C. L. (1998). The granular structure of C-type pea starch and its role in gelatinization. *Biopolymers*, 45, 323–332.

Boggracheva, T. Y., Wang, Y. L., & Hedley, C. L. (2001). The effect of water content on the ordered/disordered structures in starches. *Biopolymers*, 58, 247–259.

Bul on, A., Colonna, P., Planchot, V., & Ball, S. (1998). Starch granules: Structure and biosynthesis. *International Journal of Biological Macromolecules*, 23, 85–112.

Bul on, A., G rard, C., Riekel, C., Vuong, R., & Chanzy, H. (1998). Details of the crystalline ultrastructure of C-starch granules revealed by synchrotron microfocus mapping. *Macromolecules*, 31, 6605–6610.

Bul on, A., Pontoire, B., Riekel, C., Chanzy, H., Helbert, W., & Vuong, R. (1997). Crystalline ultrastructure of starch granules revealed by synchrotron-radiation microdiffraction mapping. *Macromolecules*, 30, 3952–3954.

Buttrose, M. S. (1960). Submicroscopic development and structure of starch granules in cereal endosperms. *Journal of Ultrastructural Research*, 4, 231–257.

Cameron, R. E., & Donald, A. M. (1992). A small-angle X-ray scattering study of the annealing and gelatinization of starch. *Polymer*, 33, 2628–2635.

Cheetham, N. W. H., & Tao, L. P. (1998). Solid state NMR studies on the structural and conformational properties of natural maize starches. *Carbohydrate Polymers*, 36, 285–292.

Dang, J. M. C., & Copeland, L. (2003). Imaging rice grains using atomic force microscopy. *Journal of Cereal Science*, 37, 165–170.

French, D. (1984). In R. L. Whistler, J. N. BeMiller, & E. F. Paschalls (Eds.), *Starch Chemistry and Technology* (pp. 183–247). New York, San Diego, CA: Academic Press.

Gidley, M. J., & Bociek, S. M. (1985). Molecular organization in starches: A  $^{13}\text{C}$  CP/MAS NMR study. *Journal of American Chemical Society*, 107, 7040–7044.

Jane, J.-L., Kasemsuwan, T., Leas, S., Zobel, H., & Robyt, F. (1994). Anthology of starch granule morphology by scanning electron microscopy. *Starch/Staerke*, 46, 121–129.

Jayakody, J., & Hoover, R. (2002). The effect of lintnerization on cereal starch granules. *Food Research International*, 35, 665–680.

Jenkins, P. J., Cameron, R. E., Donald, A. M., Bras, W., Derbyshire, G. E., Mant, G. R., et al. (1994). In situ simultaneous small and wide angle X-ray scattering: A new technique to study starch gelatinization. *Journal of Polymer Science Part B: Polymer Physics*, 32, 1579–1583.

Jenkins, P. J., & Donald, A. M. (1997). The effect of acid hydrolysis on native starch granule structure. *Starch/Staerke*, 49, 262–267.

Nikuni, Z., & Whistler, R. L. (1957). Unusual structures in corn starch granules. *Journal of Biochemistry*, 44, 227–231.

Oostergetel, G. T., & van Bruggen, E. F. G. (1989). On the origin of a low angle spacing in starch. *Starch/Staerke*, 41, 331–335.

Paris, M., Bizot, H., Emery, J., Buzare, J. Y., & Buleon, A. (1999). Crystallinity and structuring role of water in native and recrystallized starches by  $^{13}\text{C}$  CP-MAS NMR spectroscopy I: spectral decomposition. *Carbohydrate Polymers*, 39, 327–339.

Putaux, J. L., Molina-Boisseau, S., Momauro, T., & Dufresne, A. (2003). Platelet nanocrystals resulting from the disruption of waxy maize starch granules by acid hydrolysis. *Biomacromolecules*, 4, 1198–1202.

Ridou, M. J., Parker, M. L., Hedley, C. L., Boggracheva, T. Y., & Morris, V. J. (2004). Atomic force microscopy of pea starch: Origins of image contrast. *Biomacromolecules*, 5, 1519–1527.

Sarko, A., & Wu, H. C. H. (1978). The crystal structures of A-, B- and C-polymorphs of amylose and starch. *Starch/Staerke*, 30, 73–78.

Tang, H. R., & Hills, B. P. (2003). Use of  $^{13}\text{C}$  MAS NMR to study domain structure and dynamics of polysaccharides in the native starch granules. *Biomacromolecules*, 4, 1269–1276.

Veregin, R. P., Fyfe, C. A., Marchessault, R. H., & Taylor, M. G. (1986). Characterization of the crystalline A and B starch polymorphs and investigation of starch crystallization by high-resolution  $^{13}\text{C}$  CP/MAS NMR. *Macromolecules*, 19, 1030–1034.

- Vermeulen, R., Goderis, B., Reynaers, H., & Delcour, J. A. (2004). Amylopectin molecular structure reflected in macromolecular organization of granular starch. *Biomacromolecules*, *5*, 1775–1786.
- Wang, S. J., Gao, W. Y., Liu, H. Y., Chen, H. X., Yu, J. G., & Xiao, P. G. (2006a). Studies on the physicochemical, morphological, thermal and crystalline properties of starches separated from different *Dioscorea opposita* cultivars. *Food Chemistry*, *99*, 38–44.
- Wang, S. J., Liu, H. Y., Gao, W. Y., Chen, H. X., Yu, J. G., & Xiao, P. G. (2006b). Characterization of new starches separated from different Chinese yam (*Dioscorea opposita* Thunb.) cultivars. *Food Chemistry*, *99*, 30–37.
- Wang, S. J., Yu, J. L., Gao, W. Y., Liu, H. Y., & Xiao, P. G. (2006c). New starches from Traditional Chinese Medicine (TCM) – Chinese yam (*Dioscorea opposita* Thunb.) cultivars. *Carbohydrate Research*, *341*, 289–293.
- Wang, S. J., Yu, J. L., Gao, W. Y., Pang, J. P., Liu, H. Y., & Yu, J. G. (2007). Granule structural changes in native Chinese Yam (*Dioscorea opposita* Thunb var Anguo) starches during acid hydrolysis. *Carbohydrate Polymers*, *69*, 286–292.
- Wang, S. J., Yu, J. L., Yu, J. G., Chen, H. X., & Pang, J. P. (2007). The effect of acid hydrolysis on morphological and crystalline properties of Rhizoma *Dioscorea* starch. *Food Hydrocolloids*, *21*, 1217–1222.
- Ziegler, G. R., Creek, J. A., & Runt, J. (2005). Spherulitic crystallization in starch as a model for starch granule initiation. *Biomacromolecules*, *6*, 1547–1554.